This is an open access article published under an ACS AuthorChoice License, which permits copying and redistribution of the article or any adaptations for non-commercial purposes.

ACS OMEGA

http://pubs.acs.org/journal/acsodf

Article

Growth Pattern, Stability, and Properties of Complexes of C_2H_5OH and nCO_2 (n = 1−5) Molecules: A Theoretical Study

Cam-Tu Dang Phan, Nguyen Thi Ai Nhung, and Nguyen Tien Trung*

Cite This: https://dx.doi.org/10.1021/acsomega.0c00948

Read Online

ACCESS | Metrics & More | Article Recommendations | Supporting Information

ABSTRACT: This work is dedicated to theoretically investigate the formation process of $C_2H_5OH\cdots nCO_2$ (n = 1−5) complexes and to shed light on the nature of interactions formed under the variation of CO_2 concentration. It is found that CO_2 molecules tend to locate around the polarized −OH group to interact with the lone pairs of the O atom. The interaction of ethanol with three CO_2 molecules ($C_2H_5OH\cdots 3CO_2$) induces the most stable structure in the sequence considered. The atoms in molecules (AIM), NCIplot, and natural bond orbital (NBO) analyses point out that the $O_{ethanol}\cdots C_{CO_2}$ tetrel bond overcomes hydrogen, chalcogen, and $CO_2\cdots CO_2$ tetrel-bonded interactions and mainly contributes to the strength of $C_2H_5OH\cdots nCO_2$ (n = 1−5) complexes. All intermolecular interactions in the examined complexes are weakly noncovalent, and their positive cooperativity is evaluated to be slightly weaker than that of CO_2 pure systems. SAPT2+ and molecular electrostatic potential (MEP) calculations indicate that the electrostatic force is the main factor underlying the attractive interplay in the complexes of C_2H_5OH and CO_2.

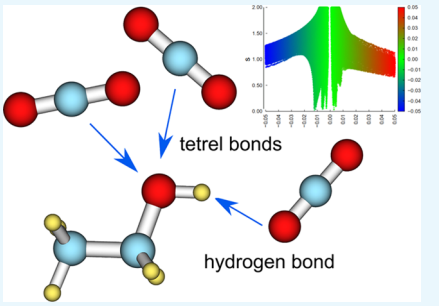

Downloaded via 14.176.225.252 on June 15, 2020 at 16:04:12 (UTC).
See https://pubs.acs.org/sharingguidelines for options on how to legitimately share published articles.

1. INTRODUCTION

The usage of supercritical carbon dioxide ($scCO_2$) was early discovered with extensive applications in nanomaterials, chemical engineering, food science, and pharmaceuticals.[1,2] Besides the understanding of thermodynamic, kinetic, and critical properties of $scCO_2$ reactions, the solubility and intermolecular interactions involving $scCO_2$ are the research subfields that attract great scientific attention because of practical applications.[3−9] Comprehensive insight into the interactions involving CO_2 at the molecular level has an important influence on improving technological applications based on $scCO_2$. Numerous studies on complexes of organic molecules and CO_2 were conducted to unveil the nature of intermolecular interactions between these molecules.[9−17] The >C/S═O···C tetrel bond was addressed as the bonding feature of binary complexes formed by carbonyl/sulfoxide compounds and CO_2.[9,11,17] This feature was also investigated for larger complexes with 2−3 CO_2 molecules.[16,18]

Many experimental investigations showed that the addition of a small amount of cosolvents into the $scCO_2$ solvent resulted in an increase in the solubility of the solutes.[19−21] In particular, some alkanes were added to $scCO_2$ to dissolve the nonpolar compounds, whereas functional organic compounds or H_2O were used for the polar ones.[22−24] Alcohols including methanol, ethanol, and propanol were extensively used as cosolvents to improve both solubility and selectivity processes.[21,24,25] According to Hosseini et al., the presence of alcohols as a cosolvent affects the shape of complexes formed, in which each alcohol has a different impact on the aggregation of CO_2 around the drugs.[24] The solubility of Disperse Red 82 and modified Disperse Yellow 119 increases substantially up to 25-fold by adding 5% of ethanol cosolvent to the $scCO_2$.[25] Vapor−liquid equilibria and critical properties of the $CO_2\cdots$ ethanol binary mixture were experimentally investigated using a variety of experimental techniques and equipment.[26−29] Becker et al. reported that the addition of CO_2 to pure ethanol leads to a decrease of interfacial tension and the adsorption of CO_2 enhances with the increasing mole fraction of CO_2 in the liquid phase.[26]

From another perspective, the behavior and origin of weak interactions such as hydrogen, tetrel, chalcogen, and halogen have been widely studied due to their considerable influence on crystal packing, material structures, and biological systems.[30−36] Besides the experimental and large-scale modeling studies of solute−solvent mixtures, a combined investigation of intermolecular interactions and ethanol solvation in $scCO_2$ helps to clarify the dissolution process and to understand its solubility for efficient and advanced applications. The great attention on binary complexes of methanol/ethanol and CO_2 was reflected through a number of articles involved.[12,37−42] From the theoretical viewpoint, the primary intermolecular interaction in the $C_2H_5OH\cdots CO_2$ complex was proposed to be the Lewis acid−base interaction

Received: March 2, 2020
Accepted: May 28, 2020

© XXXX American Chemical Society

or electron donor−acceptor one.[12,37,38] For the aggregation of CO_2 around ethanol, molecular dynamics simulations of the ethanol···64CO_2 system under supercritical conditions showed the higher probability of CO_2 around the oxygen lone pairs.[38] Some stable structures of ethanol with 1−4 and 6 molecules of CO_2 were proposed;[40] however, the growth mechanism of stable $C_2H_5OH\cdots nCO_2$ structures under addition of CO_2 molecules and geometric behaviors, energetic characteristics, and bonding features of these complexes have not been reported yet. To shed light on these unclear points, we increased the size of these complexes by adding 1−5 CO_2 guests to the ethanol host molecule and systematically investigated the growth pattern of geometry and all of the important changes of stability and electronic properties of intermolecular interactions.

2. RESULTS AND DISCUSSION

2.1. Structural Pattern of the $C_2H_5OH\cdots nCO_2$ (n = 1−5) Complexes. The stable configurations and geometric parameters of $C_2H_5OH\cdots nCO_2$ (n = 1−5) complexes at the MP2/6-311++G(2d,2p) level are presented in Figure 1a,b. The dashed lines in Figure 1a,b represent the intermolecular interactions, which are taken from AIM topological analysis. The molecular graphs of some complexes are provided in Figure S1 of the Supporting Information (SI), with the aim of finding out intermolecular interactions formed. The existence of bond critical points (BCPs) is considered to be the indicator for the formation of interactions. From Figure 1a,b, it can be observed that the geometries adopted by interactions between ethanol and nCO_2 molecules are consistent with Saitow et al.'s work,[40] who reported that the high attractive energy of ethanol in $scCO_2$ was driven by the large negative charge on the oxygen atom of ethanol (O8). Values of $\rho(r)$, $\nabla^2(\rho(r))$, and $H(r)$ at BCPs of intermolecular interactions are summarized in Table S1 of SI. These values lie in the ranges of 0.003−0.013, 0.012−0.052, and 0.001−0.002 au, respectively, indicating that all interactions formed are weakly noncovalent.[69]

For binary complexes, two types of geometries are observed: (i) tetrel-bonded model (**1A**-anti/gauche) and (ii) hydrogen-bonded one (**1B**-anti/gauche). In particular, the anti and gauche structures are formed from the corresponding anti and gauche isomers of ethanol, which are distinguished by the orientation of the OH bond with respect to the CCO plane. The anti conformer of ethanol is predicted to be more stable than the gauche one by 0.5 kcal·mol^{-1} at CCSD(T)/aug-cc-pVTZ.[43] The O8···C_{CO_2} distances of **1A**-anti and **1A**-gauche are very close to those in previous studies.[38,37] The calculated rotational constants of these structures are given in Table 1. Our predicted rotational spectra of **1A**-anti fit well with the experimental data (cf. Table 1), as previous studies did.[12,37,38,40]

When the number of CO_2 molecules increases, multiple interactions between C_2H_5OH and CO_2 molecules are observed. Indeed, six ternary structures are determined to be the minima on potential energy surfaces (PESs) of $C_2H_5OH\cdots 2CO_2$. Previous studies suggested the **2A**-anti complex as the minima for the $C_2H_5OH\cdots 2CO_2$ system,[38,40] while the gauche conformer and other four ternary complexes have not been reported so far. As shown in Figure 1a, **2A**-anti and **2A**-gauche are the rearrangements of corresponding conformers of C_2H_5OH and two CO_2 molecules via two O8···C tetrel bonds and C−H···O hydrogen bonds. It is worth noting that

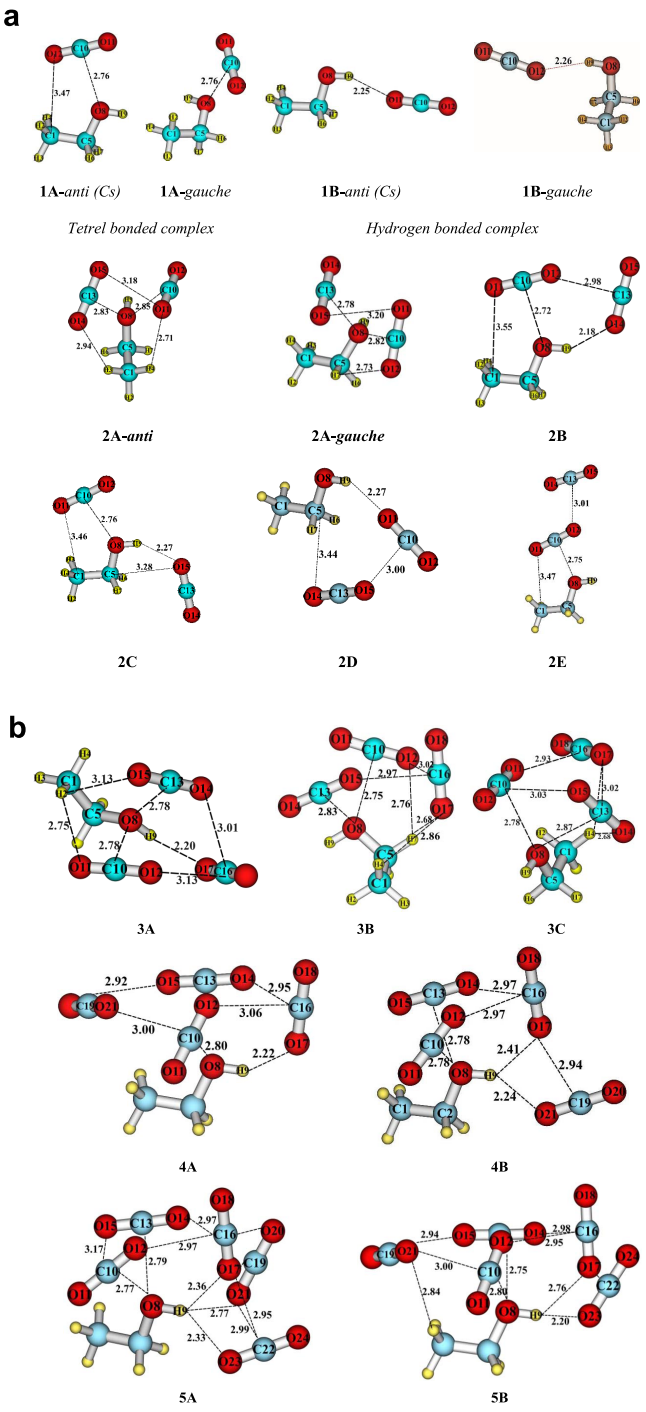

Figure 1. (a) Optimized structures of $C_2H_5OH\cdots nCO_2$ (n = 1, 2). (b) Optimized structures of $C_2H_5OH\cdots nCO_2$ (n = 3, 4, 5).

two CO_2 in **2A** are oriented to associate with two electron lone pairs of the oxygen atom O8 in C_2H_5OH. This result confirms the geometrical arrangements reported previously using molecular dynamics simulations.[38] The **2B**−**D** structures are mainly formed via O−H···O hydrogen bonds, whereas three components in **2E** associate as layers from C_2H_5OH to the first CO_2 and next to the remaining CO_2.

For n = 3−4, the stable shapes of complexes are positioned out-of-plane of CO_2 (out-of-plane here means that the O-C-O axis of CO_2 does not lie on the CCO plane of C_2H_5OH) (cf. Figure 1b). Interestingly, all submolecules interact with one another to form cage structures. The complexes with 3CO_2 are

https://dx.doi.org/10.1021/acsomega.0c00948
ACS Omega XXXX, XXX, XXX−XXX

Table 1. Rotational Constant and Vibrational Frequencies of the OH Group of Isolated Ethanol and $C_2H_5OH\cdots nCO_2$ Complexes

	A (MHz)	B (MHz)	C (MHz)		ν_{OH} (cm^{-1})	intensity ($10^{-40}\cdot esu^2\cdot cm^2$)
1A-anti	6090.39	1721.79	1365.04	C_2H_5OH	3881	38.1
1A-gauche	5989.29	1706.24	1526.29	**1A**-anti	3876	42.6
1B-anti	18475.91	0807.35	0781.04	**2A**-anti	3866	42.9
1B-gauche	8652.14	1024.63	0951.94	**3A**	3857	124.1
Exptl[38]	6128.02	1677.25	1340.85	**4A**	3852	164.5
				5A	3858	127.8

obtained from the corresponding **2A**-anti or **2A**-gauche geometries with different positions of the third CO_2. For the conformers containing four CO_2 molecules, the fourth CO_2 molecule is likely to connect to neighbor CO_2 molecules rather than the C_2H_5OH as observed in the smaller complexes with $\leq 3CO_2$ molecules. The same way is also found for stable structures with five CO_2 molecules. Complexes of ethanol with nCO_2 (n = 1−5) seem to be similar to other carbonyl-containing molecules, in which CO_2 molecules surround the functional groups (═O, >C═O, and −OH) of the host molecules.[16,44] From the optimized geometries, it is suggested that CO_2 prefers to orient around the −OH functional group to interact with the lone pair or negative region of O8 of ethanol.

2.2. Complex Stability and Changes of OH Stretching Frequency and Intensity under Variation of CO_2 Molecules. The energetic characteristics of the $C_2H_5OH\cdots nCO_2$ (n = 1−5) complexes at MP2/aug-cc-pVTZ//MP2/6-311++G(2d,2p) are gathered in Table 2. The binding energies

Table 2. Binding Energy (E_b) of $C_2H_5OH\cdots nCO_2$ (n = 1−5) Complexes (in kJ·mol^{-1}) Calculated at the MP2/aug-cc-pVTZ//MP2/6-311++G(2d,2p) level of theory

complexes	E_b	complexes	E_b
1A-anti	−11.4	**3A**	−38.2
1A-gauche	−10.7	**3B**	−35.6
1B-anti	−5.1	**3C**	−34.3
1B-gauche	−4.6	**4A**	−48.6
2A-anti	−23.9	**4B**	−47.9
2A-gauche	−23.6	**5A**	−61.9
2B	−22.1	**5B**	−59.7
2C	−17.0		
2D	−12.5		
2E	−16.2		

with zero-point energy (ZPE) and basis set superposition error (BSSE) corrections are generally negative, in the range between −4.6 kJ·mol^{-1} of the **1B** complex and −61.9 kJ·mol^{-1} of the **5A** one. Their stabilities increase in the order $1CO_2 < 2CO_2 < 3CO_2 < 4CO_2 < 5CO_2$. It is proposed that the addition of CO_2 molecules leads to the stability enhancement of investigated complexes.

As shown in Table 2, the binding energies of **1A**-anti and **1A**-gauche complexes are −11.4 and −10.7 kJ·mol^{-1}, respectively. These values are more negative than those of hydrogen-bonded structures by 5.6−6.8 kJ·mol^{-1}. Hence, the tetrel-bonded model is the energy-favorable structure of $C_2H_5OH\cdots 1CO_2$ in comparison with the hydrogen-bonded one, which is consistent with the previous static analyses.[37,40−42] Both anti isomers are found to be more negative than the gauche ones by 0.5−0.7 kJ·mol^{-1}. Thus, the anti-type geometry corresponds to the characteristic structure for ethanol complexes that exhibits large attractive energy. The electron density at BCPs adopted from AIM calculations is considered as a diagnostic of bond strength, in which a larger $\rho(r)$ value means a stronger strength and vice versa, for the same type of interaction.[45,46] The $\rho(r)$ values at BCP of the O8···C tetrel bond in **1A**-anti and **1A**-gauche are 0.010 and 0.011 au, respectively (ca. Table S1 of SI). Nevertheless, **1A**-anti is reinforced by a C═O···C1 secondary tetrel bond with $\rho(rc)$ at a BCP of 0.004 au. Therefore, the slightly higher stability of **1A**-anti as compared to **1A**-gauche is due to an additional role of the C═O···C1 tetrel bond. For comparison with some previous reports, the interaction of CO_2 with ethanol is weaker than that with carbonyl/sulfoxide compounds, approximating to that with methanol, methylamine, and obviously stronger than alkanes such as methane, ethane and ethylene.[6,8−10,16,40]

For complexes with $2CO_2$ molecules, **2A** conformers display the approximate binding energies. The remaining complexes are less stable than **2A** by roughly 1.5−7.7 kJ·mol^{-1}. The increasing stability of ternary complexes is estimated in the order of **2D** < **2E** < **2C** < **2B** < **2A**-gauche ≈ **2A**-anti. Combined with their geometries, the tetrel bonds between CO_2 and ethanol are still preferred in the case of $2CO_2$ molecules. For comparison purposes, the geometrical and energetic calculations on complexes of $(CO_2)_n$ (n = 2−3) were employed at the same level of theory in the present work. The minima and their binding energies were previously elucidated.[47−49] The calculated binding energies for the minima of these complexes are −4.4 and −12.3 kJ·mol^{-1} for $(CO_2)_2$ and $(CO_2)_3$, respectively. Both of them are less negative than those of relevant complexes between ethanol and 1, 2 molecules of CO_2 (**1A**-anti and **2A**-anti). Hence, the solvent−solvent interactions between CO_2 molecules are obviously less stable than the solute−solvent ones between CO_2 and ethanol.

To evaluate the stability and role of interaction contributing to the strength of complexes of $C_2H_5OH\cdots nCO_2$ (with n = 1, 2) as compared to those of the complexes of ethanol dimers, ethanol dimers with CO_2, computations on these complexes were performed at MP2/aug-cc-pVTZ//MP2/6-311++G(2d,2p) (details are given in the SI section). The ethanol dimer,[50−54] which were studied using both theoretical and experimental approaches, are 9 kJ·mol^{-1} more stable than the binary complexes of ethanol and CO_2. The reason for this is the stronger strength of the O−H···O hydrogen bond in ethanol dimers as compared to that of the C···O tetrel bond in $C_2H_5OH\cdots CO_2$ complexes. For $(ethanol)_2\cdots CO_2$ complexes, the stable configurations are presented in Figure S2 of SI. Their binding energies range from −16.6 to −17.9 kJ·mol^{-1} at MP2/aug-cc-pVTZ//MP2/6-311++G(2d,2p), indicating that these complexes are more stable than those formed by interaction of ethanol with $2CO_2$ molecules. It is noted that

https://dx.doi.org/10.1021/acsomega.0c00948
ACS Omega XXXX, XXX, XXX−XXX

the tetrel and/or hydrogen bonds play an important role in stabilizing the complexes considered.

Going to $3CO_2$ systems, their binding energies are significantly more negative than those of complexes involving $1,2CO_2$ molecules. The **3A** complex is the global minimum of the $C_2H_5OH\cdots 3CO_2$ system, while the **3C** one is the most weakly bound complex with binding energies of −38.2 and −34.3 kJ·mol^{-1}, respectively. All stable structures of the $3CO_2$ system found in this study are more stable than those reported by Kajiya and Saitow by around 1−6 kJ·mol^{-1} in relative energy at 6-311++G(2d,2p).[40] The complexes of C_2H_5OH with 4, $5CO_2$ have binding energies in the range of −47.9 to −61.9 kJ·mol^{-1}. This implies that the complex stabilization is enhanced when the CO_2 guest molecule is added to the previous ethanol host complex. The electron density at BCP of the $C_{CO2}\cdots$O8 contact changes insignificantly when going from n = 1 to 5 (cf. Table S1). To evaluate the cooperativity in the ternary complexes of ethanol with $2CO_2$ and compare with that of the $(CO_2)_3$ trimer, the cooperativity energies of **2A**-anti and $(CO_2)_3$ were computed using the many-body procedure.[55] These values are estimated to be −7.8 and −8.6 kJ·mol^{-1}, respectively, indicating the larger positive cooperativity of the $(CO_2)_3$ trimer as compared to that of **2A**-anti. The positive cooperativity contributes an amount of roughly 30% to the binding energy of **2A**-anti; however, it increases up to 70% in the case of the $(CO_2)_3$ trimer. Accordingly, the positive cooperativity effect plays a vital role in the formation of the $(CO_2)_3$ trimer, and its contribution is much smaller in the binding of ethanol and $2CO_2$ molecules. This finding of $C_2H_5OH\cdots nCO_2$ (n = 1−5) complexes is consistent with the positive cooperativity in other complexes stabilized by tetrel bonds.[56,57] On the basis of the energy-preferred structures, the minimum structures follow an addition pathway in which the structure with nCO_2 is built from the previous one with $(n-1)$ CO_2. The geometric formation and energetic data also reveal the important role of the oxygen site of ethanol in attracting CO_2 molecules, as previously found in complexes of carbonyl compounds with CO_2.[16,44]

To understand in more detail the stability of complexes with the increasing number of CO_2 molecules, the binding energy per CO_2 (ΔE_n) is used as a scoring for the average strength of interactions formed by the C_2H_5OH host and nCO_2 guest molecules. The changes of ΔE_n with different basis sets are presented in Figure 2. The magnitude of ΔE_n values is estimated to decrease from n = 1 and get minima at n = 3, and then, it increases with n = 4 and 5. Let us consider the **3A** structure, where two CO_2 molecules are located at the electron n-pair of oxygen and the last CO_2 molecule associates with O−H to form a hydrogen bond. In other words, the contribution of the O atom of ethanol gradually increases from n = 1 and gains the maximum with n = 3. The fourth and fifth CO_2 molecules tend to connect to other CO_2 molecules instead of ethanol to establish an ethanol:4, $5CO_2$ system. It proves the potential ability of ethanol to bind with three molecules of CO_2.

The changes of the OH stretching mode along with the addition of CO_2 are also considered in Table 1. A red shift varying from 5 to 19 cm^{-1} is observed in the stretching mode of the OH group in complexes compared to that of isolated C_2H_5OH. The ν_{OH} stretching mode of ethanol interacting with $1CO_2$ molecule was previously reported to be lower than that of isolated ethanol and consistent with the experimental results.[37] For n = 2 and 3, the ν_{OH} stretching modes of

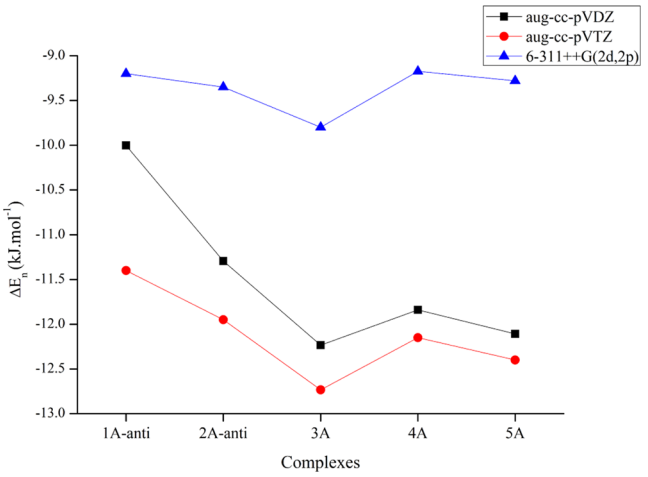

Figure 2. Binding energies per carbon dioxide.

$C_2H_5OH\cdots nCO_2$ are found to be remarkably decreased by 9−10 cm^{-1} as compared to the corresponding values with $(n-1)CO_2$. The vibrational intensity also shows an increase, up to 126.4 ($\times 10^{-40}$·esu^2·cm^2). The intensity of OH mode is significantly enhanced from 42.9 at n = 2 to 124.1 ($\times 10^{-40}$·esu^2·cm^2) at n = 3. This result is another evidence for the relatively strong interactions of ethanol with 3 molecules of CO_2. Thus, from a solvent perspective, the concentration ratio of 1:3 between ethanol and $scCO_2$ is predicted to be a potential ratio for good solubility.

2.3. Intermolecular Interaction Analysis. NCI two-dimensional (2D) and three-dimensional (3D) plots of $C_2H_5OH\cdots nCO_2$ (n = 1−5) complexes are shown in Figure 3. The low-density and low reduced gradient in the negative region of the λ_2 eigenvalue of all 2D plots demonstrate the weak and noncovalent attractive interactions between ethanol and CO_2 molecules. To further understand the difference of properties between tetrel and hydrogen bonds, 2D plots of **1A**-anti and **1B**-anti are considered. In two cases, the attractive interactions between C_2H_5OH and CO_2 are observed, which obviously dominate the repulsive interactions and are consistent with the results of Kajiya and Saitow.[40] The 2D plot of **1A**-anti has a peak in the negative region of sign $(\lambda_2)\cdot\rho(r)$ with an electron density of about 0.01 au, confirming again the noncovalent attractive nature of the O8···C tetrel bond, which was also assessed from AIM analysis. The larger volume of gradient isosurface of **1A**-anti describes a stronger strength of the O8···C tetrel bond as compared to the O−H···O hydrogen one of **1B**-anti. Furthermore, as expected, the $C1\cdots O_{CO2}$ bond is also detected via the isosurface between O of CO_2 and C of ethanol. From n = 1 to 3, the spikes expand in the negative region of sign$(\lambda_2)\cdot\rho(r)$, indicating the increase of the attractive interactions contributing to the stabilization of the corresponding complexes (cf. (a-d) of Figure 3). However, for complexes with n = 4−5, it is observed that the attractive spikes remain unchanged as compared to those of complex of $3CO_2$ (cf. (e, f) of Figure 3). It confirms the higher stability of complexes with $3CO_2$ in the sequence of 1−5 CO_2.

To identify the characteristics of intermolecular interactions and evaluate the strength of interactions, the NBO calculations were conducted at the ωB97X-D/aug-cc-pVTZ level of theory. The charge of C_2H_5OH unit, orbital interactions, and their donor−acceptor stabilization energies ($E^{(2)}$) are collected in Table 3. The other intermolecular components found in the

https://dx.doi.org/10.1021/acsomega.0c00948
ACS Omega XXXX, XXX, XXX−XXX

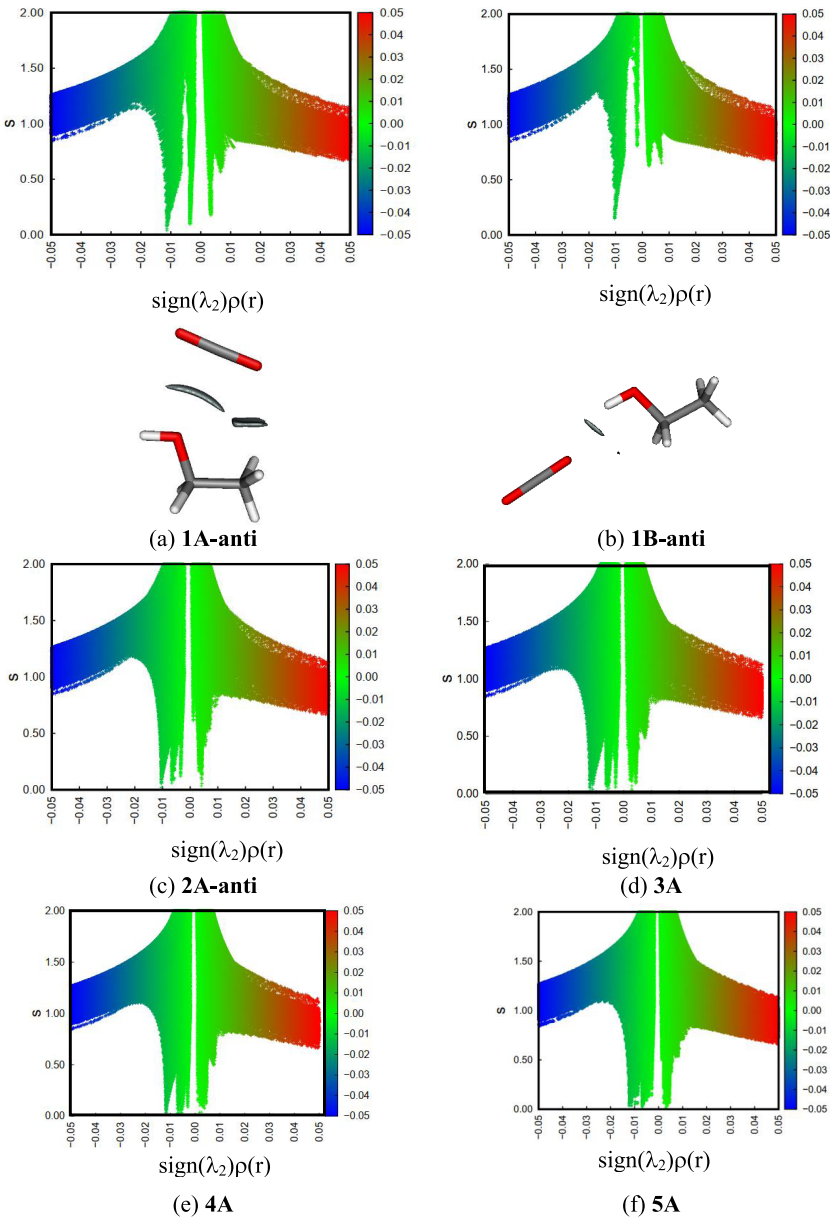

Figure 3. NCIplots of $C_2H_5OH\cdots nCO_2$ (n = 1−5) complexes (gradient isosurface of s = 0.65): (a, b) tetrel and hydrogen models of the $C_2H_5OH\cdots 1CO_2$ binary complex; (c−f) NCIplot of the most stable configurations of $C_2H_5OH\cdots nCO_2$ (n = 2−5) complexes at the MP2/6-311++G(2d,2p) level of theory.

NBO analysis with the $E^{(2)}$ values lower than 0.5 kJ·mol^{-1} are not discussed here.

In general, second-order energies of n(O8) → π^*(C═O) are significantly higher than those of other delocalization processes, revealing the decisive role of the O8···C_{CO_2} tetrel bond from an orbital perspective. For complexes of $1CO_2$, $E^{(2)}(n(O8) \rightarrow \pi^*(C{=}O))$ values of **1A**-anti and **1A**-gauche are estimated to be 6.0 and 7.3 kJ·mol^{-1}, respectively. An additive contact from a nucleophilic section π(C═O) to an electrophilic one σ^*(C−H) of the **1A**-anti complex is found with an $E^{(2)}$ of 1.0 kJ·mol^{-1}. Furthermore, the second-order interactions of n(O8) → π^*(C═O) are significantly higher than those of n(O11) → σ^*(O8−H9) by 2.3−3.3 kJ·mol^{-1}. This emphasizes the dominant role of the C···O8 tetrel bond relative to that of the O8−H9···O11 hydrogen bond in stabilizing the complexes investigated.

For the most stable complexes, the positive charge values of the C_2H_5OH unit are observed, indicating that a fraction of electronic charge is transferred from the C_2H_5OH host to the CO_2 guest molecule (cf. Table 3), in line with the attractive factor of the O site of ethanol. As a consequence, C_2H_5OH behaves as an electron donor (Lewis base), while CO_2 molecules prefer to be electron acceptor (Lewis acid) upon complexation. A small charge transfer is observed, and the electrostatic force is expected to drive intermolecular interactions.

2.4. Role of Physical Energetic Components. To further explore the contribution of the different energetic components to the total stabilization energy of the complexes, the SAPT2+ calculations are performed to separate the interaction energy into exchange, electrostatic, induction, and dispersion terms as given in Figure 4. A significantly large role of the attractive electrostatic term is observed in comparison

https://dx.doi.org/10.1021/acsomega.0c00948
ACS Omega XXXX, XXX, XXX−XXX

Table 3. NBO Analysis of $C_2H_5OH\cdots nCO_2$ (n = 1−5) Complexes at ωB97X-D/aug-cc-pVTZ

complexes	charge[a] (me)	orbital interactions	$E^{(2)}$ (kJ·mol^{-1})
1A-anti	2.44	n(O8) → π^*(C10−O12)	6.0
		π(C10−O12) → σ^*(C1−H3)	1.1
1A-gauche	3.45	n(O8) → π^*(C10−O11)	7.3
1B-anti	−0.38	n(O11) → σ^*(O8−H9)	3.7
1B-gauche	−3.03	n(O11) → σ^*(O8−H9)	8.1
2A-anti	4.49	n(O8) → π^*(C10−O12)	5.7
		n(O8) → π^*(C13−O14)	5.4
		n(O11) → π^*(C13−O14)	1.6
		n(O15) → π^*(C10−O12)	3.0
		n(O14) → σ^*(C1−H3)	0.5
2A-gauche	5.61	n(O8) → π^*(C10−O12)	5.6
		n(O8) → π^*(C13−O14)	7.4
		n(O11) → π^*(C13−O14)	2.0
		n(O15) → π^*(C10−O12)	2.1
3A	5.11	n(O8) → π^*(C10−O11)	8.6
		n(O8) → π^*(C13−O15)	5.9
		n(O17) → σ^*(O8−H9)	6.7
		n(O12) → π^*(C13−O15)	3.1
		n(O12) → π^*(C16−O18)	2.6
		n(O14) → π^*(C16−O18)	2.8
4A	4.98	n(O8) → π^*(C10−O11)	9.7
		n(O8) → π^*(C13−O15)	8.0
		n(O17) → σ^*(O8−H9)	4.5
		n(O12) → π^*(C13−O15)	2.3
		n(O12) → π^*(C16−O18)	3.2
		n(O14) → π^*(C16−O18)	4.0
		n(O15) → π^*(C19−O20)	2.1
		n(O21) → π^*(C10−O11)	3.4
5A	2.72	n(O8) → π^*(C10−O11)	8.0
		n(O8) → π^*(C13−O15)	6.8
		n(O12) → π^*(C13−O15)	3.3
		n(O12) → π^*(C16−O18)	3.1
		n(O14) → π^*(C16−O18)	3.4
		n(O14) → π^*(C19−O20)	3.1
		n(O17) → σ^*(O8−H9)	2.5
		n(O17) → π^*(C19−O20)	3.9
		n(O17) → π^*(C22−O24)	2.0

[a]Charge of C_2H_5OH unit.

with induction and dispersion terms. It is speculated that the electrostatic component acts as a prime contributor of 49−57% to the binding of $C_2H_5OH\cdots nCO_2$ complexes. The dispersion force also provides a large percentage of 35−38% to the overall stabilization, while the contribution of induction energy is only 10−12%.

The molecular electrostatic potential (MEP) is also an important tool to determine intermolecular interactions. The MEPs of monomers are displayed in Figure 5, where red regions correspond to the maximal negative potentials and blue regions indicate positive ones. Values of charges at the surface of monomers are represented by different colors, with the potentials increasing in the following order: red < orange < yellow < green < blue. All negative potentials are associated with the oxygen atoms, while the positive potentials are mainly located at C of CO_2 and H atoms of C_2H_5OH. It is accounted for the formation of the O···C═O, O−H···O, and C−H···O contacts in $C_2H_5OH\cdots nCO_2$ (n = 1−5) complexes. It is worth noting that the C atom of CO_2 and the O atom of C_2H_5OH

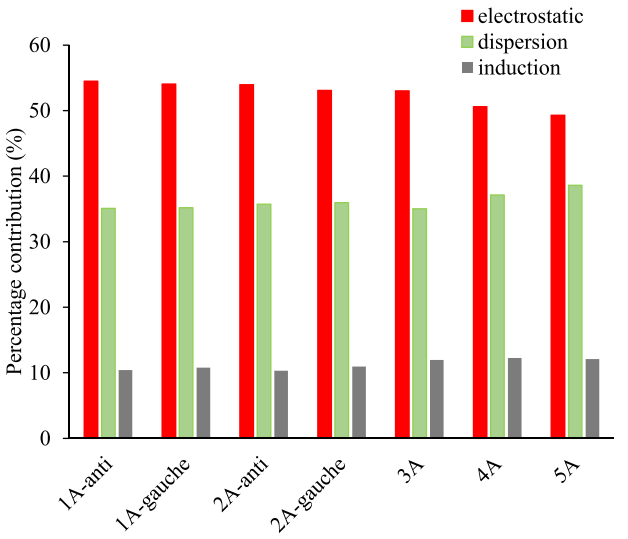

Figure 4. Contributions (%) of different energetic components to stabilization energy at MP2/aug-cc-pVDZ.

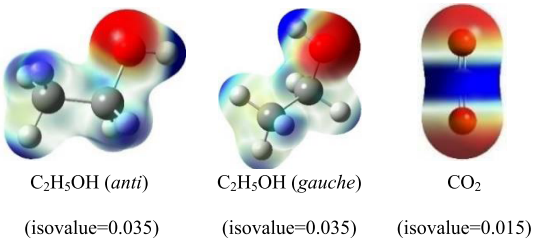

Figure 5. MEP surface of monomers at MP2/aug-cc-pVTZ.

possess the maximum of positive and negative potentials, respectively, compared to other locations in corresponding monomers. These results prove that the bonding feature of $C_2H_5OH\cdots nCO_2$ (n = 1−5) systems is the $O_{ethanol}\cdots C_{CO_2}$ tetrel bond and all intermolecular interactions are mainly held by the electrostatic attraction.

3. CONCLUSIVE REMARKS

Based on the high-level computations on $C_2H_5OH\cdots nCO_2$ (n = 1−5) systems, seventeen stable structures are found, in which CO_2 molecules preferentially solvate around −OH of ethanol as the solvation site. The obtained results are in agreement with previous studies of the equilibrium configurations of small complexes (n = 1−2); however, the stable geometries of larger complexes with n = 3−5 are discovered for the first time and exhibit an increasing trend of stability. A growth pattern in geometry is found that the stable complexes are formed based on the structures of (n − 1) CO_2 ones when adding a CO_2 molecule, with an exception of n = 5.

The binding energies with ZPE and BSSE corrections range from −4.6 to −61.9 kJ·mol^{-1} at MP2/aug-cc-pVTZ//MP2/6-311++G(2d,2p) for the complexes investigated. It is noted that the binding of C_2H_5OH with 3 CO_2 molecules has a remarkable stability, which is expected for the good solubility of ethanol in the $scCO_2$ solvent at ratio 1:3.

The weakly noncovalent nature of intermolecular interactions between C_2H_5OH and CO_2 molecules is elucidated by means of different approaches including AIM, NBO, and NCI. It is found that the positive cooperativity between the noncovalent interactions in $C_2H_5OH\cdots 2CO_2$ is slightly weaker

https://dx.doi.org/10.1021/acsomega.0c00948
ACS Omega XXXX, XXX, XXX−XXX

than that of $(CO_2)_3$ pure systems. With the addition of CO_2 molecules, the C···O tetrel bond overwhelming the C/O−H··· O hydrogen bonds is still retained as the bonding characteristic and mainly contributes to the strength of $C_2H_5OH···nCO_2$ complexes. SAPT2+ and MEP results present the major role of electrostatic energy overcoming the dispersion and induction terms in stabilizing the complexes. These findings are expected to be useful for understanding ethanol solvation in $scCO_2$.

4. COMPUTATIONAL METHODS

In this work, the geometric structures of complexes were optimized using second-order Moller−Plesset perturbation theory[58] (MP2) in combination with the 6-311++G(2d,2p) basis set. The initial geometries with a given n were built by considering all possible arrangements of the $(n - 1)$ ones and addition of one more CO_2 molecule.

The frequency calculations were performed after the geometrical optimizations to check whether the obtained structures are energetic minima on potential energy surfaces (PESs) and to compute the zero-point energy (ZPE). The binding energy ($\mathbf{E_b}$) was calculated using the MP2 method in conjunction with different basis sets including 6-311++G-(2d,2p) and aug-cc-pVXZ (X = D, T) based on the supramolecular method.[59] These values are defined as the difference in total electronic energy between the optimized complexes and the sum of two optimized monomers. The MP2 treatment that takes electron correlation into account in concert with these large basis sets has demonstrated their accuracy for noncovalent bonds in a number of studies.[60−62] The basis set superposition error (BSSE) using the counterpoise procedure[63] was also applied to evaluate the binding. To investigate the stability of these complexes with respect to the number of CO_2 molecules, the binding energy per CO_2 molecule ($\mathbf{\Delta}E_n$, n is the number of CO_2 molecules) was calculated for the most stable structures of different complex sizes using the equation

$$\Delta E_n = \frac{E_b}{n}$$

The atoms in molecules (AIM) approach[64] was applied to find evidence for formed interactions via the bond critical points (BCPs) and their local properties. Data of these analyses are taken from the AIMall package.[65] To be more specific, the positive values of Laplacian $(\nabla^2\rho(r))$ and electron energy density $(H(r))$ imply that the kinetic electron energy density $(G(r))$ is greater than the potential electron energy density $(V(r))$ and hence such interactions are characterized as closed shell or noncovalent in nature. To further identify the noncovalent behaviors, interactions between carbon dioxide and ethanol were assessed with the noncovalent interaction index (NCIplot) at MP2/6-311++G(2d,2p). NCIplot is an effective tool to detect noncovalent interactions in the real space based on electron density and reduced gradient density (s).[66,67] The value of $\mathrm{sign}(\lambda_2)\rho(r)$ is used as an effective indicator to distinguish the interactions: $\mathrm{sign}(\lambda_2)\rho(r) > 0$ indicating a repulsive interaction (nonbonding), $\mathrm{sign}(\lambda_2)\rho(r) < 0$ meaning an attractive interaction (bonding), and a value close to zero implying a very weak, van der Waals interaction. The natural bond orbital (NBO) theory along with the NBO 5.G program[68] was employed to quantitatively evaluate the charge transfer interactions between individual orbitals and the unit charges.[69] In this study, NBO analyses were performed with the ωB97X-D functional in conjunction with the Dunning aug-cc-pVTZ basis set. This functional is used instead of MP2 because the second-order perturbation energy is only generated by a well-defined one-electron Hamiltonian operator. The molecular electrostatic potential (MEP)[70] of isolated monomers was plotted at the MP2/aug-cc-pVTZ level. All quantum calculations mentioned above were carried out via the Gaussian09 package.[71]

The contribution of physical components including exchange, electrostatic, dispersion, and induction terms to the stability of complexes was determined based on the symmetry-adapted perturbation (SAPT) approach[72] because the nature of interactions could be revealed through the percentage of each one. SAPT2+ calculations were performed using density-fitted integrals, MP2 natural orbital approximation, and the aug-cc-pVDZ basis set via the PSI4 program.[73]

■ ASSOCIATED CONTENT

Supporting Information

The Supporting Information is available free of charge at https://pubs.acs.org/doi/10.1021/acsomega.0c00948.

Topological geometries of stable complexes plotted at MP2/6-311++G(2d,2p); selected parameters at BCPs of intermolecular interactions taken from calculations by means of the AIMALL package; detail of calculations and results on ethanol dimers and $(ethanol)_2···CO_2$ complexes (PDF)

■ AUTHOR INFORMATION

Corresponding Author

Nguyen Tien Trung − *Laboratory of Computational Chemistry and Modelling (LCCM), Department of Chemistry, Quy Nhon University, Quy Nhon City 590000, Vietnam;* orcid.org/0000-0001-5710-5776; Email: nguyentientrung@qnu.edu.vn

Authors

Cam-Tu Dang Phan − *Laboratory of Computational Chemistry and Modelling (LCCM), Department of Chemistry, Quy Nhon University, Quy Nhon City 590000, Vietnam*

Nguyen Thi Ai Nhung − *Department of Chemistry, University of Sciences, Hue University, Hue City 530000, Vietnam*

Complete contact information is available at: https://pubs.acs.org/10.1021/acsomega.0c00948

Notes

The authors declare no competing financial interest.

■ ACKNOWLEDGMENTS

This research is funded by Vietnam National Foundation for Science and Technology Development (NAFOSTED) under grant number 104.06-2017.11.

■ REFERENCES

(1) Reverchon, E.; Marco, I. D. Supercritical fluid extraction and fractionation of natural matter. *J. Supercrit. Fluids* **2006**, *38*, 146−166.

(2) Herrero, M.; Cifuentes, A.; Ibanez, E. Sub- and supercritical fluid extraction of functional ingredients from different natural sources: Plants, food-by-products, algae and microalgae—A review. *Food Chem.* **2006**, *98*, 136−148.

(3) Raveendran, P.; Wallen, S. L. Cooperative C−H···O hydrogen bonding in CO_2 − Lewis base complexes: Implications for solvation in supercritical CO_2. *J. Am. Chem. Soc.* **2002**, *124*, 12590−12599.

(4) Cabaço, M. I.; Danten, Y.; Tassaing, T.; Longelin, S.; Besnard, M. Raman spectroscopy of CO_2-acetone and CO_2-ethanol complexes. *Chem. Phys. Lett.* **2005**, *413*, 258−262.
(5) Kanakubo, M.; Aizawa, T.; Kawakami, T.; Sato, O.; Ikushima, Y.; Hatakeda, K.; Saito, N. Studies on solute-solvent interactions in gaseous and supercritical carbon dioxide by high-pressure 1H NMR spectroscopy. *J. Phys. Chem. B* **2000**, *104*, 2749−2758.
(6) Trung, N. T.; Nguyen, M. T. Interactions of carbon dioxide with model organic molecules: A comparative theoretical study. *Chem. Phys. Lett.* **2013**, *581*, 10−15.
(7) Li, G.; Zhou, D.; Xu, Q. Q.; Qiao, G. Y.; Yin, J. Z. Solubility of ionic liquid [Bmim]Ac in supercritical co2 containing different cosolvents. *J. Chem. Eng. Data* **2018**, *63*, 1596−1602.
(8) Kim, K. H.; Kim, Y. Theoretical studies for Lewis acid−base interactions and C−H···O weak hydrogen bonding in various CO_2 complexes. *J. Phys. Chem. A* **2008**, *112*, 1596−1603.
(9) Khanh, P. N.; Cam-Tu, P. D.; Dai, Q. H.; Quan, V. V.; Ngan, V. T.; Nguyen, M. T.; Trung, N. T. Insights into the cooperativity between multiple interactions of dimethyl sulfoxide with carbon dioxide and water. *J. Comput. Chem.* **2019**, *40*, 464−474.
(10) Diep, P.; Jordan, K. D.; Johnson, J. K.; Beckman, E. J. CO_2−Fluorocarbon and CO_2−Hydrocarbon interactions from first-principles calculations. *J. Phys. Chem. A* **1998**, *102*, 2231−2236.
(11) Rivelino, R. Lewis acid−base interactions in weakly bound formaldehyde complexes with CO_2, HCN, and FCN: Considerations on the cooperative H-bonding effects. *J. Phys. Chem. A* **2008**, *112*, 161−165.
(12) Danten, Y.; Tassaing, T.; Besnard, M. Vibrational spectra of CO_2-electron donor−acceptor complexes from ab initio. *J. Phys. Chem. A* **2002**, *106*, 11831−11840.
(13) Trung, N. T.; Hung, N. P.; Hue, T. T.; Nguyen, M. T. Existence of both blue-shifting hydrogen bond and Lewis acid−base interaction in the complexes of carbonyls and thiocarbonyls with carbon dioxide. *Phys. Chem. Chem. Phys.* **2011**, *13*, 14033−14042.
(14) Dai, H. Q.; Tri, N. N.; Trang, N. T. T.; Trung, N. T. Remarkable effects of substitution on stability of complexes and origin of the C−H···O(N) hydrogen bonds formed between acetone's derivative and CO_2, XCN (X = F, Cl, Br). *RSC. Adv.* **2014**, *4*, 13901−13908.
(15) Ingrosso, F.; Ruiz-López, M. F. Electronic interactions in iminophosphorane superbase complexes with carbon dioxide. *J. Phys. Chem. A* **2018**, *122*, 1764−1770.
(16) Azofra, L. M.; Scheiner, S. Tetrel, chalcogen and CH···O hydrogen bonds in complexes of paring carbonyl- containing molecules with 1, 2, 3 molecules of CO_2. *J. Chem. Phys.* **2015**, *142*, 1−9.
(17) Altarsha, M.; Ingrosso, F.; Ruiz-López, M. F. A new glimpse into the CO_2-Philicity of carbonyl compounds. *Chem. Phys. Chem.* **2012**, *13*, 3397−3403.
(18) Cam-Tu, P. D.; Ngan, V. T.; Trung, N. T. General trends in structure, stability and role of interactions in the complexes of acetone and thioacetone with carbon dioxide and water. *Chem. Phys.* **2020**, *530*, 110580−110587.
(19) Wu, W.; Zhang, J.; Han, B.; Chen, J.; Liu, Z.; Jiang, T.; He, J.; Li, W. Solubility of room-temperature ionic liquid in supercritical CO_2 with and without organic compounds. *Chem. Commun.* **2003**, *9*, 1412−1413.
(20) Wu, W.; Li, W.; Han, B.; Jiang, T.; Shen, D.; Zhang, Z.; Sun, D.; Wang, B. Effect of organic cosolvents on the solubility of ionic liquids in supercritical CO_2. *J. Chem. Eng. Data* **2004**, *49*, 1597−1601.
(21) Zhang, Z.; Wu, W.; Liu, Z.; Han, B.; Gao, H.; Jiang, T. A study of tri-phasic behavior of ionic liquid−methanol−CO_2 systems at elevated pressures. *Phys. Chem. Chem. Phys.* **2004**, *6*, 2352−2357.
(22) Dobbs, J. M.; Wong, J. M.; Johnston, K. P. Nonpolar co-solvents for solubility enhancement in supercritical fluid carbon dioxide. *J. Chem. Eng. Data* **1986**, *31*, 303−308.
(23) Walsh, J. M.; Ikonomou, G. D.; Donohue, M. D. Supercritical phase behavior: The entrainer effect. *Fluid Phase Equilib.* **1987**, *33*, 295−314.
(24) Hosseini, S. Z.; Bozorgmehr, M. R.; Masrurnia, M.; Beyramabadi, S. A. Study of the effects of methanol, ethanol and propanol alcohols as Cosolvents on the interaction of methimazole, propranolol and phenazopyridine with carbon dioxide in supercritical conditions by molecular dynamics. *J. Supercrit. Fluids* **2018**, *140*, 91−100.
(25) Lee, M. J.; Ho, C. C.; Lin, H. M.; Wang, P. Y.; Lu, J. S. Solubility of Disperse Red 82 and modified Disperse Yellow 119 in supercritical carbon dioxide or nitrous oxide with ethanol as a cosolvent. *J. Supercrit. Fluids* **2014**, *95*, 258−264.
(26) Becker, S.; Werth, S.; Horsch, M.; Langenbach, K.; Hasse, H. Interfacial tension and adsorption in the binary system ethanol and carbon dioxide: Experiments, molecular simulation and density gradient theory. *Fluid Phase Equilib.* **2016**, *427*, 476−487.
(27) Yoon, J. H.; Lee, H. S.; Lee, H. High-pressure vapor-liquid equilibria for carbon dioxide + methanol, carbon dioxide + ethanol, and carbon dioxide + methanol + ethanol. *J. Chem. Eng. Data* **1993**, *38*, 53−55.
(28) Yeo, S. D.; Park, S. J.; Kim, J. W.; Kim, J. C. Critical properties of carbon dioxide + methanol, + ethanol, +1-propanol, and + 1-butanol. *J. Chem. Eng. Data* **2000**, *45*, 932−935.
(29) Stievano, M.; Elvassore, N. High-pressure density and vapor−liquid equilibrium for the binary systems carbon dioxide−ethanol, carbon dioxide−acetone and carbon dioxide−dichloromethane. *J. Supercrit. Fluids* **2005**, *33*, 7−14.
(30) Dunitz, J. D.; Gavezzotti, A. How molecules stick together in organic crystals: weak intermolecular interactions. *Chem. Soc. Rev.* **2009**, *38*, 2622−2633.
(31) Volkert, L. G.; Conrad, M. The role of weak interactions in biological systems: The dual dynamics model. *J. Theor. Biol.* **1998**, *193*, 287−306.
(32) Scheiner, S. Ability of IR and NMR spectral data to distinguish between a tetrel bond and a hydrogen bond. *J. Phys. Chem. A* **2018**, *122*, 7852−7862.
(33) Bene, J. E. D.; Alkorta, I.; Elguero, J. Potential energy surfaces of HN(CH)SX:CO_2 for X = F, Cl, NC, CN, CCH, and H: N···C tetrel bonds and O···S chalcogen bonds. *J. Phys. Chem. A* **2019**, *123*, 7270−7277.
(34) Southern, S. A.; Bryce, D. L. NMR investigations of noncovalent carbon tetrel bonds. Computational assessment and initial experimental observation. *J. Phys. Chem. A* **2015**, *119*, 11891−11899.
(35) Brammer, L. Halogen bonding, chalcogen bonding, pnictogen bonding, tetrel bonding: origins, current status and discussion. *Faraday Discuss.* **2017**, *203*, 485−507.
(36) Anthony, L. C. Tetrel, pnictogen and chalcogen bonds identified in the gas phase before they had names: a systematic look at non-covalent interactions. *Phys. Chem. Chem. Phys.* **2017**, *19*, 14884−14896.
(37) Lalanne, P.; Tassaing, T.; Danten, T. Y.; Cansell, F.; Tucker, S. C.; Besnard, M. CO_2-ethanol interaction studied by vibrational spectroscopy in supercritical CO_2. *J. Phys. Chem. A* **2004**, *108*, 2617−2624.
(38) Saharay, M.; Balasubramanian, S. Electron donor-acceptor interactions in ethanol-CO_2 mixtures: an Ab initio molecular dynamics study of supercritical carbon dioxide. *J. Phys. Chem. B* **2006**, *110*, 3782−3790.
(39) McGuire, B. A.; Martin−Drumel, M. A.; McCarthy, M. C. Electron donor−acceptor nature of the ethanol−CO_2 dimer. *J. Phys. Chem. A* **2017**, *121*, 6283−6287.
(40) Kajiya, D.; Saitow, K. Significant difference in attractive energies of C_2H_6 and C_2H_5OH in $scCO_2$. *J. Supercrit. Fluids* **2017**, *120*, 328−334.
(41) Xu, W.; Yang, J.; Hu, Y. Microscopic structure and interaction analysis for supercritical carbon dioxide−ethanol mixtures: A Monte Carlo simulation study. *J. Phys. Chem. B* **2009**, *113*, 4781−4789.
(42) Skarmoutsos, I.; Guardia, E.; Samios, J. Hydrogen bond, electron donor-acceptor dimer, and residence dynamics in supercritical CO_2-ethanol mixtures and the effect of hydrogen bonding on

https://dx.doi.org/10.1021/acsomega.0c00948
ACS Omega XXXX, XXX, XXX−XXX

single reorientational and translational dynamics: A molecular dynamics simulation study. *J. Chem. Phys.* **2010**, *133*, No. 014504.
(43) Scheiner, S.; Seybold, P. G. Quantum chemical analysis of the energetics of the *anti* and *gauche* conformers of ethanol. *Struct. Chem.* **2009**, *20*, 43−48.
(44) Kajiya, D.; Imanishi, M.; Saitow, K. Solvation of esters and ketones in supercritical CO_2. *Phys. Chem. B* **2016**, *120*, 785−792.
(45) Bader, R. F. W. Atoms in Molecules. In *Encyclopedia of Computational Chemistry*; John Wiley & Sons, Ltd, 2002.
(46) Bentley, J. Behavior of electron density functions in molecular interaction. *J. Phys. Chem. A* **1998**, *102*, 6043−6051.
(47) Illies, A. J.; McKee, M. L.; Schelgel, H. B. Ab initio study of the carbon dioxide dimer and the carbon dioxide ion complexes [(CO2)2+ and (CO2)3+]. *J. Phys. Chem. A* **1987**, *91*, 3489−3494.
(48) Nesbitt, D. J. High-resolution infrared spectroscopy of weakly bound molecular complexes. *Chem. Rev.* **1988**, *88*, 843−870.
(49) Tsuzuki, S.; Klopper, W.; Luthi, H. P. High-level ab initio computations of structures and relative energies of two isomers of the CO_2 trimer. *J. Chem. Phys.* **1999**, *111*, 3846−3854.
(50) Dyczmons, V. Dimers of Ethanol. *J. Phys. Chem. A* **2004**, *108*, 2080−2086.
(51) Hearn, J. P. I.; Cobley, R. V.; Howard, B. J. High-resolution spectroscopy of induced chiral dimers: A study of the dimers of ethanol by Fourier transform microwave spectroscopy. *J. Chem. Phys.* **2005**, *123*, No. 134324.
(52) Emmeluth, C.; Dyczmons, V.; Kinzel, T.; Botschwina, P.; Suhm, M. A.; Yáñez, M. Combined jet relaxation and quantum chemical study of the pairing preferences of ethanol. *Phys. Chem. Chem. Phys.* **2005**, *7*, 991−997.
(53) Vargas-Caamal, A.; Ortiz-Chi, F.; Moreno, D.; Restrepo, A.; Merino, G.; Cabellos, J. L. The rich and complex potential energy surface of the ethanol dimer. *Theor. Chem. Acc.* **2015**, *134*, No. 1834.
(54) Finneran, I. A.; Carroll, P. B.; Mead, G. J.; Blake, G. A. Hydrogen bond competition in the ethanol−methanol dimer. *Phys. Chem. Chem. Phys.* **2016**, *18*, 22565−22572.
(55) Xantheas, S. S. Ab initio studies of cyclic water clusters $(H_2O)_n$, n = 1−6. II. Analysis of many-body interactions. *J. Chem. Phys.* **1994**, *100*, 7523−7534.
(56) Marín-Luna, M.; Alkorta, I.; Elguero, J. Cooperativity in tetrel bonds. *J. Phys. Chem. A* **2016**, *120*, 648−656.
(57) Anila, S.; Suresh, C. H. Formation of large clusters of CO_2 around anions: DFT study reveals cooperative CO_2 adsorption. *Phys. Chem. Chem. Phys.* **2019**, *21*, 23143−23153.
(58) Møller, C.; Plesset, M. S. Note on an approximation treatment for many-electron systems. *Phys. Rev.* **1934**, *46*, 618−622.
(59) Morokuma, K.; Kitaura, K. *Variational Approach (SCF ab initio calculations) to the Study of Molecular Interactions: the Origin of Molecular Interactions, in Molecular Interactions*; Ratajczak, H.; Orville-Thomas, W. J., Eds.; Wiley: New York, 1980.
(60) El Kerdawy, A.; Murray, J. S.; Politzer, P.; Bleiziffer, P.; Heßelmann, A.; Görling, A.; Clark, T. Directional noncovalent interactions: repulsion and dispersion. *J. Chem. Theory Comput.* **2013**, *9*, 2264−2275.
(61) Alkorta, I.; Elguero, J.; Del Bene, J. E. Azines as electron-pair donors to CO_2 for N···C tetrel bonds. *J. Phys. Chem. A* **2017**, *121*, 8017−8025.
(62) Del Bene, J. E.; Alkorta, I.; Elguero, J. What Types of noncovalent bonds stabilize dimers $(XCP)_2$, for X = CN, Cl, F, and H? *J. Phys. Chem. A* **2019**, *123*, 10086−10094.
(63) Boys, S. F.; Bernardi, F. The calculation of small molecular interactions by the differences of separate total energies. Some procedures with reduced errors. *Mol. Phys.* **1970**, *19*, 553−566.
(64) Bader, R. F. W. A quantum theory of molecular structure and its applications. *Chem. Rev.* **1991**, *91*, 893−928.
(65) Keith, T. A. *TK Gristmill Software*; AIMAll: Overland Park KS, USA, 2019. aim.tkgristmill.com.
(66) Johnson, E. R.; Keinan, S.; Mori-Sánchez, P.; Contreras-García, J.; Cohen, A. J.; Yang, W. Revealing noncovalent interactions. *J. Am. Chem. Soc.* **2010**, *132*, 6498−6506.
(67) Contreras-García, J.; Johnson, E. R.; Keinan, S.; Chaudret, R.; Piquemal, J. P.; Beratan, D. N.; Yang, W. NCIPLOT: A program for plotting noncovalent interaction regions. *J. Chem. Theory Comput.* **2011**, *7*, 625−632.
(68) Glendening, E. D.; Badenhoop, J. K.; Reed, A. E.; Carpenter, J. E.; Bohmann, J. A.; Morales, C. M.; Weinhold, F. *NBO 5.G; Theoretical Chemistry Institute*; University of Wisconsin: Madison, 1996−2001.
(69) Glendening, E. D.; Landis, C. R.; Weinhold, F. Natural bond orbital methods. *Wiley Interdiscip. Rev.: Comput. Mol. Sci.* **2012**, *2*, 1−42.
(70) Murray, J. S.; Politzer, P. The electrostatic potential: an overview. *Wiley Interdiscip. Rev.: Comput. Mol. Sci.* **2011**, *1*, 153−163.
(71) Frisch, M. J.et al. *Gaussian 09*; Gaussian Inc.: Wallingford, CT, 2009.
(72) Jeziorski, B.; Moszynski, R.; Szalewicz, K. Perturbation theory approach to intermolecular potential energy surfaces of van der Waals complexes. *Chem. Rev.* **1994**, *94*, 1887−1930.
(73) Parrish, R. M.; Burns, L. A.; Smith, D. G. A.; Simmonett, A. C.; dePrince, A. E.; Hohenstein, E. G.; Bozkaya, U.; Sokolov, A. U.; Remigio, R. D.; Richard, R. M.; Gonthier, J. F.; James, A. M.; McAlexander, H. R.; Kumar, A.; Saitow, M.; Wang, X.; Pritchard, B. P.; Verma, P.; Schaefer, H. F.; Patkowski, K.; King, R. A.; Valeev, E. F.; Evangelista, F. A.; Turney, J. M.; Crawford, T. D.; Sherrill, C. D. Psi4 1.1: An open-source electronic structure program emphasizing automation, advanced libraries, and interoperability. *J. Chem. Theory Comput.* **2017**, *13*, 3185−3197.

https://dx.doi.org/10.1021/acsomega.0c00948
ACS Omega XXXX, XXX, XXX−XXX